Customizing Structure–Function Displacements in the Macula for Individual Differences

Andrew Turpin,[1] Siyuan Chen,[1] Juan A. Sepulveda,[2] and Allison M. McKendrick[2]

[1]Department of Computing and Information Systems, The University of Melbourne, Melbourne, Australia
[2]Department of Optometry and Vision Sciences, The University of Melbourne, Melbourne, Australia

Correspondence: Andrew Turpin, Department of Computing and Information Systems, University of Melbourne, Parkville VIC 3010, Australia; aturpin@unimelb.edu.au.

Submitted: January 1, 2015
Accepted: July 27, 2015

Citation: Turpin A, Chen S, Sepulveda JA, McKendrick AM. Customizing structure–function displacements in the macula for individual differences. *Invest Ophthalmol Vis Sci*. 2015;56:5984–5989. DOI:10.1167/iovs.15-17384

Purpose. In the macula, retinal ganglion cells (RGCs) are displaced from their receptive fields. We used optical coherence tomography (OCT) to customize displacements for individual eyes by taking into account macular shape parameters, and determined the likely effect of individual anatomical differences on structure–function mapping in the central visual field.

Methods. Using the population average model of Drasdo et al. as a starting point, we altered the RGC count in that model based on the ratio of an individual's RGC layer plus inner plexiform layer thickness to the population average on a pointwise basis as a function of eccentricity from the fovea. For 20 adults (age, 24–33; median age, 28) with normal vision, we computed displacements with the original model and our customized approach. We report the variance in displacements among individuals and compare the effects of such displacements on structure–function mapping of the commonly used the 10-2 visual field pattern.

Results. As expected, customizing the displacement using individual OCT data made only a small difference on average from the population-based values predicted by the Drasdo et al. model. However, the range between individuals was over 1° at many locations, and closer to 2° at some locations in the superior visual field.

Conclusions. Individualizing macular displacement measurements based on OCT data for an individual can result in large spatial shifts in the retinal area corresponding to 10-2 locations, which may be important for clinical structure–function analysis when performed on a local, spatial scale.

Keywords: macula, optical coherence tomography, visual function, glaucoma

Recent studies have highlighted the importance of macular assessment for the detection of glaucoma.[1–4] One important clinical method for detecting and monitoring glaucoma is the comparison of structural measures of the retina, such as data provided by optical coherence tomography (OCT) scans, to visual function measures, such as those provided by a visual field examination. Hood and Raza[5] suggest that diagnostic precision can be increased by examining the thickness of the retinal ganglion cell plus inner plexiform layers (RGC+) and retinal nerve fiber layer (RNFL) as measured by OCT in local regions where visual field abnormalities occur. For any such localized structure–function comparison, an accurate correspondence between visual field locations and locations in the OCT data is needed.

However, in the context of glaucoma (or other ganglion cell disorder), there is not a simple, direct concordance between a location in a visual field test and a location on the retina in the macular region, because the retinal ganglion cell (RGC) bodies are displaced from their receptive fields. Several research groups have actively studied the size of the displacement across the macular region,[6–9] and others have applied these data to adjust visual field locations to account for the displacement of RGCs when examining structure–function relationships in the macula.[10,11]

Existing models ignore variations in RGC displacement between individuals, instead they predict an average RGC displacement computed based on population data. They are based on a simple counting argument,[8] with the direction of the displacement of RGCs from their receptive fields assumed to be radial and directly away from the fovea, with the magnitude of the displacement such that the number of receptive fields and the number of RGCs are equal at the location in question along that radial. In turn, this assumes a fixed distribution of RGCs and receptors for all people along any given radial. The major recent work in the area has been in attempting to estimate these RGC and receptor distributions.[6,7,12]

Spectral-domain OCT technology now allows high resolution images of the retina; in particular, allowing quantification of the thickness of RNFL and RGC+ in an individual. By comparing this thickness to the population average, it is possible to adjust the distribution of RGCs for that individual in the models that compute RGC body displacement. For example, if an individual's RGC+ is thicker than the population average near the macula, we would infer that the individual has more RGCs than average closer to the macula. If we then assume that the number of RGC receptive fields is relatively constant among individuals (assuming younger healthy adults with normal vision), this must mean that the displacement of the RGCs from the receptors is shorter than average for this individual. This is the intuition behind our individualization of displacement calculations.

We computed individual displacements in 20 individuals for locations in the well-known 10-2 visual field test pattern used

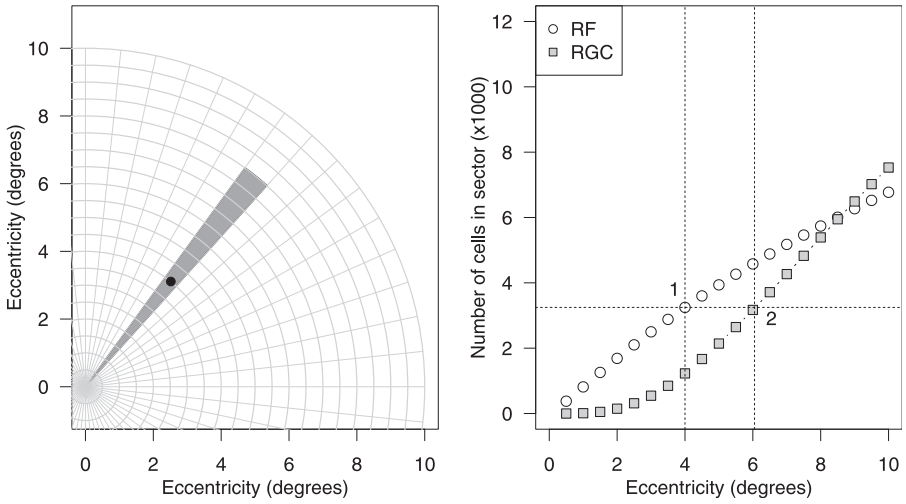

Figure 1. Our implementation of the model of Drasdo et al.[6] For a retinal location (*black point* in *left*), the number of receptive fields in the sector containing the location (*shaded grey* in *left*) is determined (point 1, *right*). Next, the lowest eccentricity where the number of RGCs in the sector is at least as large as the number of receptive fields is located (point 2, *right*). The displacement is the difference between this eccentricity and the eccentricity of the original location ($6.05 - 4 = 2.05°$ in this example).

by the Humphrey Field Analyzer (Carl Zeiss Meditec, Inc., Dublin, CA, USA). By examining the variation in displacement for these individuals, we can form predictions regarding whether such customized mapping may be worthwhile in a clinical setting.

Methods

Computing Models

We began with the model of Drasdo et al.[6] (see the Appendix for details), which calculates the average displacement of RGCs from their receptive fields, and is shown schematically in Figure 1. For a given location in the macula, we first computed the number of receptive fields in a thin sector radiating from the center of the macula to the location (plotted as the open-circle curve in the right of Fig. 1), and then computed the number of RGCs (the grey-square curve of Fig. 1). This calculation is based on empirical data that gives the density of each cell type at various eccentricities,[6,8] which is converted into cell counts by tiling the retina with small patches along the radial of interest, as plotted in the left of Figure 1. The distance between *x*-axis locations where these two curves share a *y*-axis value indicates that there is a 1-to-1 relationship between RGCs and receptive fields, thus giving displacements, as shown in the right of Figure 1.

The density of RGCs was computed by natural neighbor interpolation of the data from Curcio and Allen.[8] This is different from the original Drasdo et al.[6] model, where the density was computed using a polynomial fitted to these same data. The density of receptive fields is given by Equation 7 of the Drasdo et al.[6] study, replicated as Equations 1 to 4 in the Appendix.

To modify the RGC count at some location on the retina for an individual, we multiplied the cell count given by the population average for a patch at that location by the ratio of the RGC+ thickness for the individual to the population average RGC+ thickness (Equation 6 in the Appendix) at that patch. In this study, RGC+ thickness was extracted from the VOL files of four radial scans centered automatically in the foveal center according to patient's fixation using the Spectralis SD-OCT (Heidelberg Engineering, Heidelberg, Germany). Each scan was obtained using a high resolution custom pattern, with an angular separation of 45° between each (0°, 45°, 90°, and 135°) and with a scan length of 20°, as shown in the top left of Figure 2. The automatic real time mean (ART) function of the Spectralis was used to obtain the maximum resolution, averaging 100 frames to obtain a resolution of 3.87 μm axial, 11.2 μm transverse, and 1.9 μm of penetration. Images with a

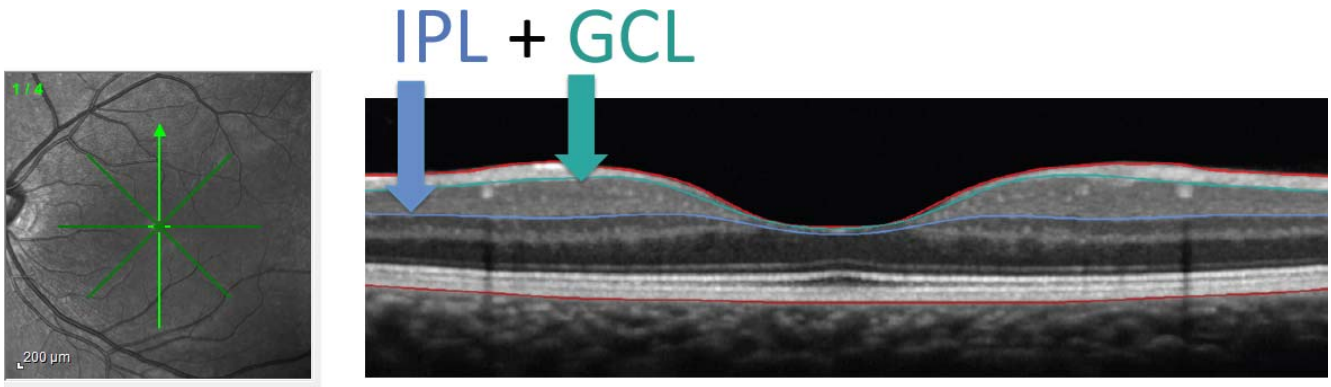

Figure 2. The retinal boundaries defined in Spectralis OCT (*right*), with radial scans at 0°, 45°, 90°, and 135° (*left*). RGC+, the sector between the boundaries of RNFL and IPL shown in this OCT image.

Investigative Ophthalmology & Visual Science

Table 1. Participant Ocular Refractive and Acuity Details

Subject	Age	Eye Tested	Axial length, mm	Refractive Error	logMAR
Y1	31	LE	23.25	−0.75	0
Y2	28	RE	24.58	−3.75/−1.00 × 45	0.1^{+2}
Y3	31	RE	24.02	Plano	−0.2
Y4	24	LE	23.6	Plano	0
Y5	27	RE	23.84	Plano	−0.1
Y6	27	LE	23.16	Plano	−0.1
Y7	26	RE	23.1	−3.25/−1.50 × 12	0
Y8	30	RE	22.52	−1.50	0.1
Y9	29	LE	23.93	−1.75/−1.00 × 0	0
Y10	32	RE	22.5	−0.5/−0.25 × 75	0
Y11	33	LE	24.13	−1.00 × 90	0
Y12	27	RE	22.82	Plano	0
Y13	24	LE	23.81	−3.25	0
Y14	28	LE	23.17	−3.25/−1.25 × 165	0^{+1}
Y15	32	LE	25.42	−3.25/−1.75 × 45	−0.1
Y16	27	LE	21.98	Plano	−0.2
Y17	27	RE	23.18	Plano	0^{-1}
Y18	29	LE	23.1	Plano	-0.1^{+2}
Y19	24	RE	22.32	−0.25/−1.25 × 15	−0.1
Y20	28	RE	22.44	−2.75/−0.5 × 175	0

quality of signal higher than 15 dB were considered for the data analysis.

Thickness of RGC+ was taken as the difference between the RNFL boundary and the IPL boundary defined by the Spectralis, as shown for an example in Figure 2, right. All automatic image segmentation was checked manually and adjusted if necessary by an author (JS) before extraction of the data. The receptive field count was not altered from the population average for each individual (see Discussion).

Participants

Data for 20 visually normal participants (7 males, 13 females), with an age ranging from 24 to 33 years (median, 28) was collected. The OCT scans collected on the 20 participants formed the "population average" RGC+ used in our analysis. For each participant, only one eye was selected randomly (10 right eye, 10 left eye). Participants were recruited from the staff, students, or via personal contacts from the Department of Optometry and Vision Sciences at the University of Melbourne.

All participants underwent a screening evaluation that consisted of a short personal history, the best corrected visual acuity and refractive error measurements, slit-lamp examination to verify media clarity, pupil size measurement in standard room lighting conditions, and an Amsler Grid test. All had refractive errors lower than ±5 diopters (D) spherical and/or −2 D cylindrical, and have no important systemic or ophthalmic disorders (such as maculopathy, important media opacities, fixation problems), and have a pupil size larger than 3 mm. Refractive error, visual acuity, and axial length data appears in the Table.

The project was approved by the University of Melbourne Human Research Ethics Committee (HREC 1238744), and all the individuals provided written informed consent in accordance with the tenants of the Declaration of Helsinki.

Measurement Results Presentation

Since different conventions regarding meridians and locations to the visual center often are used for retina anatomy and visual field presentations, to avoid confusion, in this study, we presented the results in the format of 10-2 visual field locations of a right eye. That is, the positive *x*-coordinates always refer to the temporal visual field of either eye in Cartesian coordinates, and the four meridians temporal, superior, nasal, inferior are in the order of the increasing polar angle in the visual field.

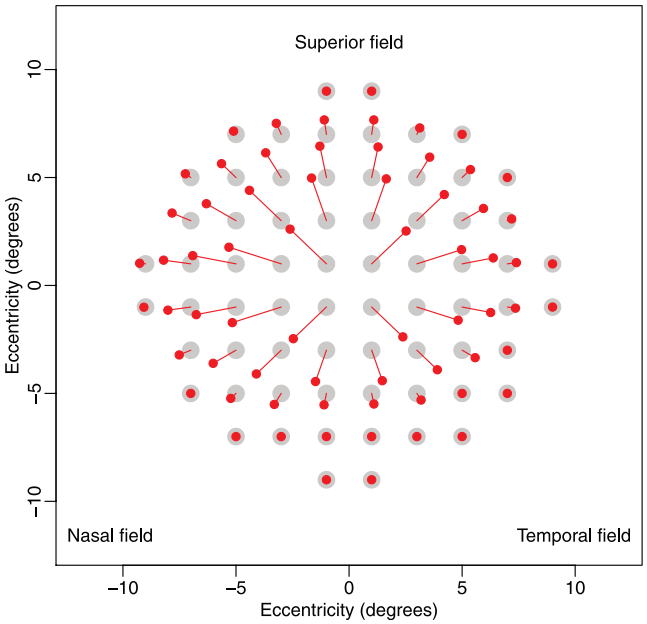

Figure 3. Population displacements, modeled by the Drasdo et al.[6] study, calculated by the RGC density, modeled in the Curcio and Allen[8] study, and receptive field density, modeled in the Drasdo et al.[6] study. For each *grey* 10-2 location, the connected *red line* leads to the displacement of that location as a *small red circle*.

Results

Figure 3 shows the population average displacements of locations in the 10-2 pattern computed using our implementation of the Drasdo et al.[6] model. The length of the solid lines represents the size of the displacement. The maximum displacement is 2.44° at location (−3°,+1°), followed by location (−3°,−1°) with a displacement of 2.28°, and then 2.27° and 2.15° displacements at (−1°,+1°) and (+1°,+1°), respectively.

Figure 4 uses a similar representation, but has a colored dot for each 10-2 location for the displacements of each of the 20 younger participants computed using our customized approach. As can be seen, there is substantial variation among individuals.

Figure 5 presents descriptive statistics of individual displacements for each location. The numerical value at each location is the average displacement (left) and the range (difference between the maximum and minimum displacement among 20 participants, right) over 20 participants. The size of the bubble at each location indicates the difference between the average displacements from our dataset to the population displacements from the Drasdo et al.[6] model, which are very small, within 0.22°. As is shown, after RGC+ ratio adjustment, the average individual displacement maximizes at (−3°,+1°) with 2.4°, followed by a displacement of 2.3° at (−1°,+1°) and (−3°,−1°), and 2.2° at (+1°,+1°). The largest range is 2.2°, occurring at (−5°,+7°), followed by 2.0° and 1.9° at (−3°,+7°) and (5°,+3°), and 1.8° at (+3°,+3°) and (−5°,+5°).

Investigative Ophthalmology & Visual Science

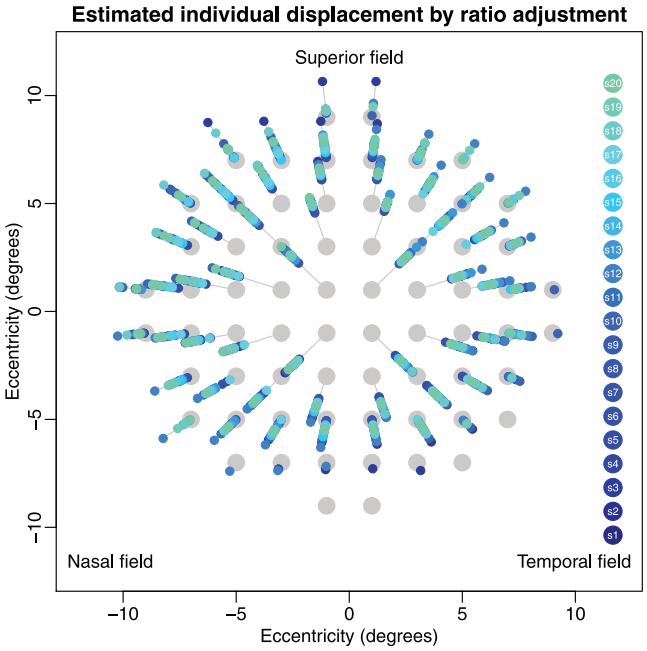

FIGURE 4. Individual displacements of 20 young participants, one color per participant) denoted by different colors, at the 10-2 test locations.

DISCUSSION

We chose to use the Curcio and Allen model[8] for RGC density and the Drasdo et al.[6] model for RGC receptive field density because these models have been used by others[10,13] to assist clinical comparison of macular OCT data to visual fields. However, other models are in the literature; for example, the model of Watson,[9] where different formulas were used for the calculation of the density of RGC and RGC receptive fields. A key difference is that the models of Watson were fitted mainly to peripheral cell counts (outside 11°), not counts in the macula (within 10°), which is the focus of this study.

Our model estimates contain some asymmetry relative to the center of the fovea. This is fairly small in the nasal/temporal meridian, but greater in the superior/inferior meridian. The results seem reasonable in that the average of our customized displacement population is similar to the average reported by Drasdo et al,[6,9] where the average displacements peaked at approximately 2.2° at the eccentricity of 1.9° in the temporal retina meridian and peaked at approximately 1.9° at the eccentricity of 2° in the nasal retina meridian. In our study, the largest displacement occurred in the 10-2 tests at the eccentricities between 1° and 3° near the four meridians. The largest average displacements in the 10-2 tests near the temporal and nasal retina regions are 2.44° and 2.15°, respectively, which are very close to the results in these studies.[6,9] Moreover, the largest displacements near the inferior and superior retina regions in our study are 2.27° and 2.07°, which are greater than the reported total displacement of 0.37 ± 0.03 mm along the vertical meridian (within 1.8°–2.9°) in the study of Sjöstrand et al.,[7] probably because of the limited number of human retinas (5 retinas) examined.

As mentioned in the Methods, receptive field estimates were obtained from previously reported functional/psychophysical data,[6] and not collected individually for our participants. They were held constant across all individuals, which is a potential weakness of this study. Given that our study population included healthy, young adults only, it did not seem that the extensive additional functional testing required to test the validity of this assumption was justified. In a population of wider age range, the assumption of consistent receptive field density is less likely to hold. Neuronal density decreases in older retinae; however, the decrease is relatively less in the macula than in other regions, so the effects of age may not be pronounced.[14] Collecting estimates of receptive field density

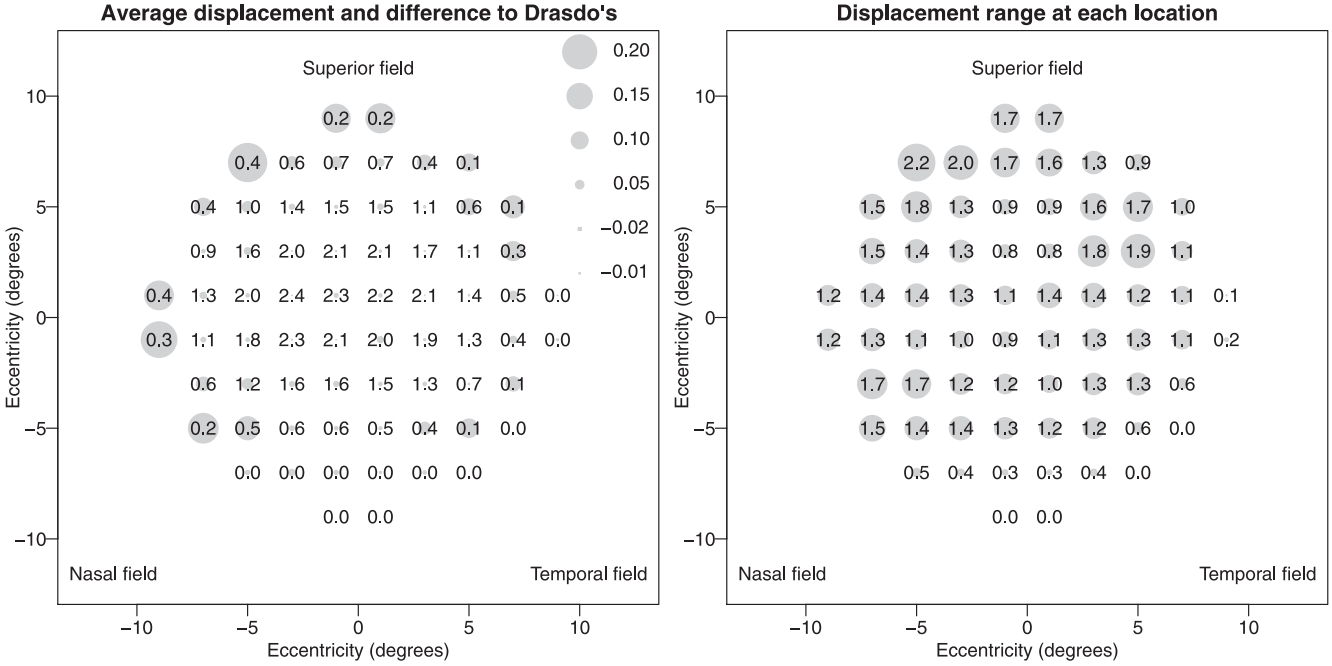

FIGURE 5. The average individual displacement (the numerical value on the *left*) and the range (the numerical value on the *right*) over 20 participants from the 10-2 test locations. The size of *circle* on the *left* indicates the difference (*solid circle* for positive difference, while *square* for negative difference) from the population displacement. The bubble size on the *right* indicates the range of individual displacement. For example, the range at (–5°,+7°) is 1.96° to 3.22° and the size of the bubble is plotted as 3.22° – 1.96° = 2.16°.

psychophysically is difficult, but obtaining individual estimates from imaging may be less laborious. One possible imaging approach could be to use the outer nuclear layer (ONL) in the OCT data to adjust receptive field counts in the same way that RGC counts are altered. However, Henle fibers comprise up to 70% of the ONL,[15] and these are the fiber lengths we are trying to model, so it seems confounded to include them in the model. Furthermore, the segmentation of the ONL layer is not as easy as the segmentation of the RGC+ layers, because of lack of contrast in this region of the OCT images, as shown in Figure 2. We did attempt some initial analyses using the ONL layer, but the results were wildly variable, and seemed unlikely to be plausible.

There are several points of clinical relevance to consider in interpreting the results of our study. Firstly, we used RGC+ thickness to individually estimate the number of RGCs at a given eccentricity. Our approach is limited to areas of healthy macula, becoming invalid once the RGC+ is thinned due to disease. Consequently, customized mapping of macular structure–function in a clinical setting would be useful only in the initial stages of the disease, or at baseline, to provide a reference point for future changes. Alternately, other individual features of macular anatomy might assist once disease is onset. One possible feature is the size of the foveal avascular zone, which has been shown to relate to macular shape in normal observers.[16] Foveal pit depth may seem like a possible candidate; however, in our data there was no significant correlation between foveal pit depth (as measured by the OCT) and displacement for 63 of the 68 visual field locations (Spearman correlations, $P > 0.05$, data not shown), so this factor is unlikely to be particularly helpful.

A second point of clinical relevance is that the largest displacements were in the inferior retina. The inferior macular area is susceptible to damage in glaucoma;[1] hence, the area most likely to be damaged also is the region that is most likely to benefit from customized mapping. In this spatial area of high clinical relevance, there is the greatest predicted interindividual difference in the mapping, of up to 2° between individuals. Given that the 10-2 visual field grid separates visual field locations by 2°, this level of individual shift in mapping is sufficient to map an area on the OCT image to different visual field test locations in different individuals. One application for such mapping may be for the exploration of the relationship between structural and function data collected in patients with glaucoma, particularly to assist in the detection and monitoring of early progression. We did not investigate structure and function in our current cohort with the two mapping schema as there is limited relationship between structural and functional data in healthy eyes.[17–19] The benefits of such mapping are unlikely to be revealed by looking at structure–function correlations averaged across a population, as most people within a population have relatively typical anatomy. Benefits of individualized mapping are most likely in those people with atypical anatomy, where individual tracking of progression may be assisted by moving away from population norms. Furthermore, customized mapping may pave the way for future visual field test grids that are individually adjusted depending on anatomical features.

Summary

We estimated individual displacements of 10-2 locations for 20 participants with normal vision by adjusting RGC counts in a model based on that of Drasdo el al.[6] using the ratio of RGC+ thickness to its population thickness. The results demonstrated that although the average individual displacement did not deviate from the population displacement, the variation among individuals was substantial, and may have implications for clinical structure–function analysis.

Acknowledgments

Supported by Australian Research Council Linkage Project LP130100055 (AT, AMM).

Disclosure: **A. Turpin**, Heidelberg Engineering GmBH (F); **S. Chen**, None; **J.A. Sepulveda**, None; **A.M. McKendrick**, Heidelberg Engineering GmBH (F)

Appendix

Computing Displacement

The following pseudo code describes our implementation of the Drasdo et al.[6] model.

1. Let $D_c(r,\theta)$ be the density of RGCs and $D_f(r,\theta)$ be the density of RGC receptive fields at some retinal location (r,θ) in polar coordinates. Both functions give density in cells/mm^2.
2. Assume we wish to estimate the displacement for receptive field location (R,θ), and that α and K are chosen so that the sector subtending α degrees centered on θ is tiled into K subsectors (as in the left panel of Figure 1).
3. Compute the number of receptive fields in the sector out to radius R mm:

$$N_f = \sum_{i=1}^{K} \frac{\alpha\pi}{360} \frac{2iR^2}{K^2} D_f(iR/K, \theta).$$

4. Compute the number of RGCs in the sector out to radius kR/K mm, for some $k \geq 1$:

$$N_c(k) = \sum_{i=1}^{k} \frac{\alpha\pi}{360} \frac{2iR^2}{K^2} D_c(iR/K, \theta).$$

This is the RGC curve in the right of Figure 1.

5. Find k so that $|N_c(k) - N_f|$ is minimized.
6. Report displacement as $kR/K - R$ mm.

In this paper, we used the equations of Drasdo et al.[6] to compute D_f, at angular eccentricity (E) as follows:

$$R_{ve}(r,\theta) = R_{v0}\left(1 + \frac{r}{E_{2v}(\theta)}\right) \quad (1)$$

$$R_{oe}(r) = R_{o0}\left(1 + \frac{r}{E_{2o}}\right) \quad (2)$$

$$k(r) = 1 + (1.004 - 0.007209r + 0.001694r^2 - 0.00003765r^3)^{-2} \quad (3)$$

$$D_f(r,\theta) = (1.12 + 0.0273r)k(r)/1.155 \Big/ \left(R_{ve}(r,\theta)^2 - R_{oe}(r)^2\right) \quad (4)$$

where R_{v0} is the visual minimum angle of resolution (MAR) at eccentricity 0°, and is set as 0.011785; R_{o0} is the optical MAR at

eccentricity 0°, set as 0.008333; E_{2o} is the eccentricity proportional to the standard deviation of the Gaussian spread function for the eye, set as 20°; E_{2v} at any eccentricity, 0 to 359 for each radial path, is the linear interpolation value between 2.19 at 0°, 1.98 at 90°, 2.26 at 180°, 1.5 at 270°, 2.19 at 360°, 1.98 at 450°.

Function D_c was computed using natural neighbor interpolation on the data of Curcio and Allan,[8] downloaded from http://www.cis.uab.edu/sloan/GanglionCellTopography/ June 2014.

Computing the Ratio for Customizing Displacement

We require the ratio between the RGC+ thickness of an individual along a given radial at any angle. This is computed using the technique of Scheibe et al.[20]

Individual RGC+ thickness along eight radial scans from the OCT data was firstly fit by the function shown in Equation 5, then the data between two radial scans were monotonically interpolated by the Steffen method,[21] allowing thickness at any location in the retina to be determined. The ratio at any eccentricity e along some radial for participant n then is calculated as the ratio of individual RGC+ thickness (RGC_n) to the population RGC+ thickness, as shown in Equation 6, where N is the number of participants. The pseudo code below describes the algorithm.

$$f(r;\mu,\sigma,\gamma,\alpha) = \mu\sigma^2 r^{\gamma}\exp[-\mu r^{\gamma}] + \alpha(1-\exp[-\mu r^{\gamma}]) \quad (5)$$

$$ratio_n(e) = \frac{RGC_n(e)}{\frac{1}{N}\sum_1^N RGC_n(e)} \quad (6)$$

1. Input segmentation data from OCT and calculate the difference between the RNFL and IPL boundaries to get RGC+ thickness curves at different radial scans.
2. Find the local minima of the curve as the foveal center for each radial scan and set the minima position as the starting point.
3. Fit the Scheibe model with Equation 5 on RGC+ curve from 0 to 2.5 mm from the foveal center.
4. Outside the radial scans, RGC+ thickness were interpolated by the Steffen method between any two radial scans.
5. After gathering 20 participants' RGC+ thickness data at each location in each radial path, calculate the ratio at each location in any radial path with Equation 6.

References

1. Hood DC, Raza AS, de Moraes CGV, Liebmann JM, Ritch R. Glaucomatous damage of the macula. *Prog Retin Eye Res*. 2013;32:1–21.
2. Ohkubo S, Higashide T, Udagawa S, et al. Focal relationship between structure and function within the central 10 degrees in glaucoma. *Invest Ophthalmol Vis Sci*. 2014;55:5269–5277.
3. Sato S, Hirooka K, Baba T, Tenkumo K, Nitta E, Shiraga F. Correlation between the ganglion cell-Inner plexiform layer thickness measured with cirrus HD-OCT and macular visual field sensitivity measured with microperimetry. *Invest Ophthalmol Vis Sci*. 2013;54:3046–3051.
4. Takahashi M, Omodaka K, Maruyama K, et al. Simulated visual fields produced from macular RNFLT data in patients with glaucoma. *Curr Eye Res*. 2013;381:1133–1141.
5. Hood DC, Raza AS. On improving the use of OCT imaging for detecting glaucomatous damage. *Br J Ophthalmol*. 2014;98: ii1–ii9.
6. Drasdo N, Millican CL, Katholi CR, Curcio CA. The length of Henle fibers in the human retina and a model of ganglion receptive field density in the visual field. *Vision Res*. 2007;47: 2901–2911.
7. Sjöstrand J, Popovic Z, Conradi N, Marshall J. Morphometric study of the displacement of retinal ganglion cells subserving cones within the human fovea. *Graefes Arch Clin Exp Ophthalmol*. 1999;237:1014–1023.
8. Curcio CA, Allen KA. Topography of ganglion cells in human retina. *J Comp Neurol*. 1990;300:5–25.
9. Watson AB. A formula for human retinal ganglion cell receptive field density as a function of visual field location. *J Vis*. 2014;14:1–17.
10. Raza AS, Cho J, de Moraes CV, et al. Retinal ganglion cell layer thickness and local visual field sensitivity in glaucoma. *Arch Ophthalmol*. 2011;129:1529–1536.
11. Hood DC, Raza AS. Method for comparing visual field defects to local RNFL and RGC damage seen on frequency domain OCT in patients with glaucoma. *Biomed Opt Express*. 2011;2: 1097–1105.
12. Curcio CA, Sloan KR, Kalina RE, Hendrickson AE. Human photoreceptor topography. *J Comp Neurol*. 1990;292:497–523.
13. Hood DC, Nguyen M, Ehrlich AC, et al. A test of a model of glaucomatous damage of the macula with high-density perimetry: implications for the locations of visual field test points. *Transl Vis Sci Technol*. 2014;3:1–10.
14. Harman A, Abrahams B, Moore S, Hoskins R. Neuronal density in the human retinal ganglion cell layer from 16-77 years. *Anat Rec*. 2000;260:124–131.
15. Curcio CA, Messinger JD, Sloan KR, Mitra A, McGwin G, Spaide RF. Human chorioretinal layer thicknesses measured in macula-wide, high-resolution histologic sections. *Invest Ophthalmol Vis Sci*. 2011;52:3943–3954.
16. Tick S, Rossant F, Ghorbel I, et al. Foveal shape and structure in a normal population. *Invest Ophthalmol Vis Sci*. 2011;52: 5105–5110.
17. Garway-Heath DF, Holder GE, Fitzke FW, Hitchings RA. Relationship between electrophysiological, psychophysical, and anatomical measurements in glaucoma. *Invest Ophthalmol Vis Sci*. 2002;43:2213–2220.
18. Redmond T, Anderson RS, Russell RA, Garway-Heath DF. Relating retinal nerve fiber layer thickness and functional estimates of ganglion cell sampling density in healthy eyes and in early glaucoma. *Invest Ophthalmol Vis Sci*. 2013;54:2153–2162.
19. Denniss J, Turpin A, McKendrick AM. Visual contrast detection cannot be predicted from surrogate measures of retinal ganglion cell number and sampling density in healthy young adults. *Invest Ophthalmol Vis Sci*. 2014;55:7804–7813.
20. Scheibe P, Lazareva A, Braumann U-D, et al. Parametric model for the 3D reconstruction of individual fovea shape from OCT data. *Exp. Eye ReS*. 2014;119:19–26.
21. Steffen M. A simple method for monotonic interpolation in one dimension. *Astron Astrophys*. 1990;239:443–450.

Investigative Ophthalmology & Visual Science